Proceedings of the ASME 2021
International Design Engineering Technical Conferences and
Computers and Information in Engineering Conference
IDETC/CIE2021
August 17 – 20, 2021, Virtual Conference, USA

DETC2021/71376

OPTIMIZED TORQUE ASSISTANCE DURING WALKING WITH AN IDEALIZED HIP EXOSKELETON

Neethan Ratnakumar
Xianlian Zhou*
Department of Biomedical Engineering
New Jersey Institute of Technology
Newark, New Jersey, 07102
Email: alexzhou@njit.edu

ABSTRACT

The hip muscles account for a great percentage of the total human energy expenditure during walking and many wearable devices have been developed in assisting the hip joint to reduce the metabolic Cost Of Transport (COT) for walking. However, the effectiveness of assisting the hip in only one direction (either flexion or extension) or both directions has not been systematically studied and the underlying muscle mechanics and energetics affected by the assistance are not well understood. In this study, human-exoskeleton simulation based optimizations were performed to find optimized hip assistance torque profiles for (1) unidirectional flexion assistance, (2) unidirectional extension assistance, and (3) bidirectional flexion and extension assistance. Our results show that the bidirectional assistance is the most effective in reducing the COT of walking (22.7% reduction) followed by flexion (19.2%) and extension (11.7%). The flexion assistance resulted in more COT saving than the output of its net work by 35.9%, which indicates that the negative work done (42.2% of its positive counterpart) also played an important role in reducing the COT. The bidirectional assistance also reduced the activations of the hip extensors to a great extent and shifted the activation pattern of the hip flexor (ilipsoas). These results can provide valuable information for optimal hip actuation (timing and profiles) and help exoskeleton designers make informed decisions.

Keywords: Hip exoskeleton; Torque Assistance; Optimization

NOMENCLATURE

DOF Degree Of Freedom
ES Early Stance
GRF Ground Reaction Force
LO Liftoff
LP Landing Preparation
LS Late Stance
MSK Musculoskeletal
COT Cost Of Transport
SSS Self Selected Speed
SW Swing

1. INTRODUCTION

The use of robotic exoskeletons to assist human motion has become one of the most promising approaches to enhance human performance or rehabilitate gait disorders in mobility impaired patients (e.g. individuals with stroke). Assistance provided to lower body joints such as the hip, knee, and ankle for walking or running has been investigated by many researchers [1]. The hip and ankle muscle tendon units perform most of the positive work in walking while the knee muscle tendons mainly serve to absorb energy [2]. The review by Sawicki et al. [1] found that thus

*Address all correspondence to this author.

far hip exoskeletons can reduce the metabolic cost during walking up to 19.8% [3], more than ankle exoskeletons (12% [4]), whereas only one knee exoskeleton has been shown to improve walking economy (during inclined walking with a backpack [5]). The hip muscles account for the greatest percentage of the total human energy expenditure during walking [6], thus torque assistance delivered to the hip joint is expected to reduce the metabolic cost of human walking to a great degree. Meanwhile, hip torque assistance can also benefit other lower leg joints such as the ankle. In the work by Lenzi et al. [7] it was shown that hip assistance alone was capable of reducing activations of ankle muscles considerably. It is also well known that extra hip work can compensate plantarflexor deficits and loss of push off strength in the ankle joint [8, 9]. Therefore, hip joint assistance can be an effective and energy efficient choice in lower-limb exoskeletons.

Within a walking stride, the hip muscles generate substantial torques for both flexion and extension with similar magnitudes [10]. There are many wearable devices that were designed to provide bidirectional assistance to the hip joint [11–19] while there are others that have been designed to only assist the hip in either flexion [20–24] or extension direction [25–28]. For cable driven or soft actuator devices [21, 25, 27], assisting only one direction could simplify the design and lower the cost considerably. However, there is no clear or conclusive evidence on which assistance direction is superior in reducing energy expenditure and muscle activity or if bidirectional assistance can have much greater advantage. Regardless of design choices, optimal assistance strategies that aim to achieve the greatest benefits to the wearers, often associated with the timing and profile of assistance, are being actively pursued.

The physical human-in-the-loop optimization protocol, an experimental procedure in which systematic alteration to the device assistance control parameters or profiles is performed based on real-time recorded human physiological data [29], has shown promise in minimizing subject-specific metabolic costs in a soft hip exosuit [27] and in an ankle device [29]. However, experimental studies with physical devices are often costly as they require substantial investment of time and resources. Despite of showing evidence of effectiveness from exoskeleton assistance, these studies often fall short of providing a full understanding or explanation of the delicate human muscle adaptation due to altered force demand and associated muscle mechanics and physiology [30].

Musculoskeletal (MSK) simulations have been utilized in estimating the effects of assistive devices on human beings in recent years [31]. Such simulations have the potential to provide insight to muscle mechanics such as muscle force, power and metabolic cost that are difficult to measure experimentally and have the ability to predict outcomes for hypothetical "what if" scenarios. Dembia et al. [32] employed the Computed Muscle Control (CMC) method to optimize idealized assistance torques to lower-limb joints with different combinations of single joint and multi-joint assistance. The biomechanical and energetic effects of ideal assistance applied to lower-limb joints during running have also been investigated using a similar approach [33]. The CMC simulation method utilizes experimental motion data from healthy subjects' normal walking or running motions (without exoskeletons) and does not account for the changes in kinematics and Ground Reaction Forces (GRFs) induced by the assistive devices. In another study by Jackson et al. [30], the effects of ankle exoskeleton assistance on metabolic rate during walking were studied with prescribed kinematics and electromyography (EMG)-driven MSK simulations. Through simulations, this study explained the unexpected observation of increased metabolic rate with increasing amounts of average exoskeleton torque. These CMC and EMG driven simulations shed light on how exoskeletons could interact with muscle mechanics and energetics but are limited by the need for experimental motion data. In the work by Zhou et al. [34, 35], predictive human-in-the-loop simulations were presented to enable the design and evaluation of a variety of exoskeletons with or without experimental data. Other simulation tools such as single shooting based optimization [36] and direct collocation based optimal control [37] provide more flexible environments for assistive device simulations.

This study investigates and compares the effects of idealized hip assistance in flexion and extension through a predictive human-in-the-loop modeling and optimization approach. We aim to investigate the optimal torque assistance profiles for hip flexion, extension, and a combination of both. By doing so, we provide clues on which assistance direction is more effective in reducing the metabolic Cost Of Transport (COT) in walking and what are the major benefits of assisting the hip in both directions. We first present the simulation and single shooting based optimization method for walking gait generation with muscle reflex control and then demonstrate muscle co-optimization with hip joint torque assistance. We then provide results and discussion on gait characteristics, muscle activation, and metabolic COT, all of which are affected by the hip torque assistance. At the end the conclusion and potential future directions are discussed.

2. MATERIALS AND METHODS

2.1 Musculoskeletal Model

To study human walking, we employed a generic musculoskeletal model included in the SCONE software [36], which is a planar reduced gait model adapted from the Gait2354 model included in the OpenSim software [38]. The model shown in Fig. 1 has nine DOFs and is actuated by sixteen Hill-type muscle tendon units [39]. The muscles include the fourteen major lower-limb muscle models employed in [40] with the addition of the bi-articulate rectus femoris muscles.The height of the model is approximately 1.8 meters and it weighs 75.165 kg. Contact spheres are positioned at the toe and the heel of each foot and a compliant

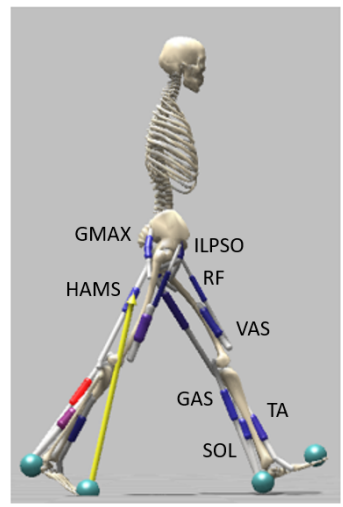

FIGURE 1: THE MUSCULOSKELETAL MODEL. IT HAS 16 MUSCLES INCLUDING: ILIOPSOAS (ILPSO), GLUTEUS MAXIMUS (GMAX), RECTUS FEMORIS (RF), HAMSTRINGS (HAMS), VASTI (VAS), GASTROCNEMIUS (GAS), TIBIALIS ANTERIOR (TA), AND SOLEUS (SOL).

Hertz/Hunt-Crossley contact model [41] was utilized to compute the contact force between each sphere and the ground.

2.2 Simulation

The walking gaits were generated through a muscle reflex based gait controller [40] whose parameters were optimized with a Covariance Matrix Adaptation Evolutionary Strategy (CMA-ES) method [42]. The optimization was conducted with the SCONE software [36], which used OpenSim [38] to execute single shooting forward dynamics simulations of walking within optimization iterations. The gait controller recognizes several sequential high-level states (phases) including early stance (ES), late stance (LS), liftoff (LO), swing (SW) and landing preparation (LP) and coordinates low level control laws for individual muscles. The ES phase starts when the foot strikes the ground. The LS phase starts when the horizontal distance between the ipsilateral (stance) foot and pelvis is smaller than 0 (i.e. the stance foot is behind the pelvis COM). The LO or pre-swing phase starts when the contralateral foot enters the ES phase. The SW phase starts when the foot is just off the ground. And the LP phase starts when the horizontal distance between the ipsilateral (swing) foot and pelvis is greater than 0 (i.e. the swing foot is in front of the pelvis COM).

In this study, the TA muscle excitation was controlled during the entire gait cycle with positive length feedback from itself and negative force feedback from the SOL. SOL and GAS muscles were controlled through the three stance states with positive force feedback. RF was controlled only during LO with positive

	ES	LS	LO	SW	LP
TA	L+				
	$F^{-}_{(SOL)}$				
SOL	F+				
GAS	F+				
VAS	F+, C (DOF knee_angle)				
RF			L+, C		
ILPSO	PD, C		L+, C	PD, L+	
				$L^{-}_{(HAMS)}$	
HAMS	PD, C			F+	
GMAX	PD, C		C	F+	

FIGURE 2: LOW-LEVEL CONTROL LAWS USED TO DETERMINE EXCITATION IN THE MUSCLES. POSITIVE AND NEGATIVE FEEDBACK ARE DENOTED BY (+) AND (-), RESPECTIVELY. ALL FEEDBACKS ARE BASED ON STATES FROM THE SAME MUSCLE, EXCEPT FOR A NEGATIVE FORCE FEEDBACK FROM THE SOLEUS TO THE TIBIALIS ANTERIOR AND A NEGATIVE LENGTH FEEDBACK FROM HAMS TO ILPSO.

length feedback plus a constant signal. The VAS was controlled by conditional muscle reflexes with positive force feedback and constant signal control laws which were active during the stance states. This conditional reflex suppresses the muscle control when the knee is in extension and the maximum knee angle is greater than a to-be-optimized angle, which prevents hyperextension of the knee during the stance states [43]. The overall low-level control laws, with mathematical equations given in [40,44], for all muscles are presented in Fig. 2, including constant signals (C), feedback from normalized muscle fiber length (L), normalized muscle-tendon force (F), and proportional-derivative (PD) control based on the pelvis tilt angle. Similar to Wang et al. [43], we did not include normalized muscle fiber velocity (V) feedback in this study.

The objective function, J, of the optimization problem was defined as a weighted combination of multiple motion characteristics, including metabolic Cost of Transport (COT) calculated as the total metabolic cost (based on an energetics model [45]) normalized by the distance traveled and the model's body mass, non-falling walking gait with a prescribed speed range, penalties for injury such as over-extension caused limit force at the knee, and joint limit violations of the ankle ($\pm 60^{\circ}$):

$$J = w_{COT} J_{COT} + w_{gait} J_{gait} + w_{injury} J_{injury} + w_{ankle} J_{ankle} \quad (1)$$

with weights $w_{COT} = 1$, $w_{gait} = 100$, $w_{injury} = 0.01$ and $w_{ankle} = 0.1$.

An optimization was first performed to generate a normal walking motion with Self Selected Speed (SSS) by specifying

only the lower limit of the walking speed at 0.75 m/s. The optimization variables for the normal walking include all the muscle reflex control parameters. Then parameterized hip joint torques (flexion/extension) were directly added to the hip joint for assistance simulations through a conditional feed forward controller. The assistance torque profile was assumed to take the form of a raise-peak-fall curve [29] and the parameters include the offset time, raise time, fall time, and the peak torque (shown in Fig. 3a). The raise and fall curves were parameterized and jointed by a sine and a cosine function at the peak. The raise and fall times was set to be between 0.05 to 0.3 seconds during optimization. The peak torque was allowed to vary between 10 Nm to 50 Nm. For flexion assistance, the reference starting time for offset is the beginning of the LS phase whereas for extension the reference time is the beginning of the LP phase.

For the case where both flexion and extension assistance were provided, an interpolatory Catmull-Rom spline was used instead. The spline, shown in Fig. 3b, was parameterized by four time intervals t_1, t_2, t_3 and t_4. The torque profile 1) starts at zero at the beginning of the LP phase (without any offset) and raises to a peak extension torque of 50 Nm at the end of t_1, 2) gradually decreases to zero at the end of time period t_2, 3) increases to a maximum flexion torque of 50 Nm at the end of period t_3, 4) decreases to zero at the end of t_4, and 5) finally remains at zero until the next LP phase begins. The start and end of the spline have both zero values and zero tangents and the middle zero value induces the transition between extension and flexion assistances. All four time intervals ($t_1 - t_4$) were optimization variables with the ranges between 0.2-0.4 seconds. An additional objective function term was added to minimize the difference between the stride duration (D) and the sum of these four time intervals in order to approximately enforce continuous assistance over the entire gait cycle. In this case the peak torque magnitudes were fixed at 50 Nm for both extension and flexion instead of treating them as optimization variables. During the simulations, these assistance parameters were optimized together with the muscle reflex parameters such that co-adaptations of muscle reflex and assistance could happen.

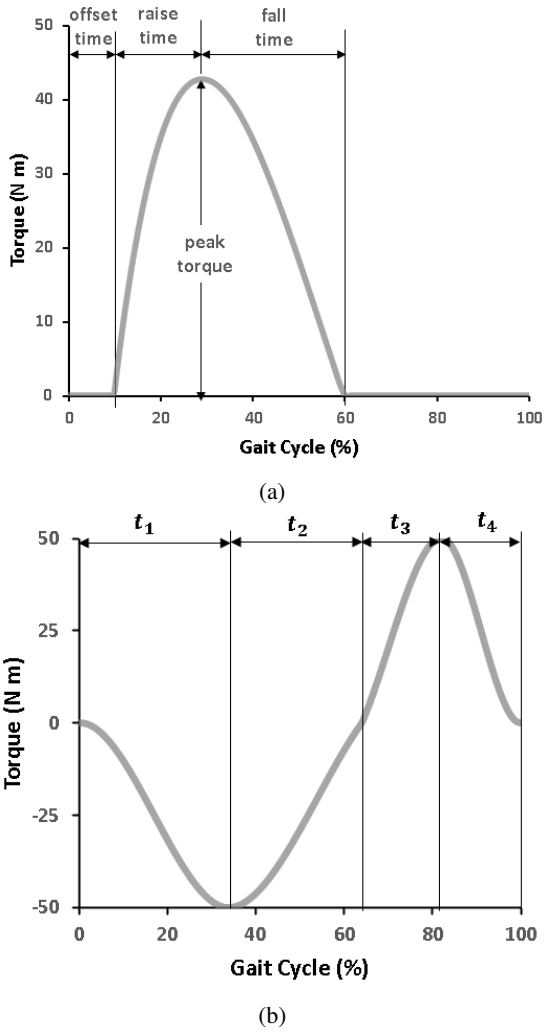

FIGURE 3: (a) PARAMETERIZATION OF HIP FLEXION ASSISTANCE TORQUE, DEFINED BY THE OFFSET TIME, RISE TIME, FALL TIME, AND PEAK TORQUE. (B) PARAMETERIZATION OF HIP EXTENSION AND FLEXION TORQUE DEFINED BY FOUR TIME INTERVALS FROM t_1 TO t_4.

3. RESULTS AND DISCUSSION

We ran multiple optimizations to generate four walking gaits of SSS for the normal walking and the assisted walking under three conditions. To find the optimal gait for each case, we used 10 second simulations and a set of 10 parallel optimizations and at the end chose the one with minimum J as the optimal solution. The gait characteristics predicted for all four walking gaits are compared in Table 1. With assistance, the SSS increased by 16.8%, 10.5% and 16.6% for the two unidirectional cases and the bidirectional case, respectively. Flexion assistance changed the stride length (L) minimally but shortened the stride duration (D) (i.e. increased step frequency). Extension assistance increased step frequency further but decreased the stride length. Like the other two assistance cases, the bidirectional case also shortened the stride length and increased the step frequency. Among the three cases, the extension assistance has the shortest stride length and highest step frequency.

The predicted hip and knee angles are shown in Fig. 4 for all cases with the hip angle ranges listed in Table 1. The hip angle pattern for unassisted walking is similar to the angles reported in adults walking at their natural speed by Bovi et al. [46], although with higher extension prior to toe-off and higher flexion during early stance. Flexion assistance caused the hip to flex much more

TABLE 1: COMPARISON OF GAIT CHARACTERISTICS FOR NORMAL AND ASSISTED WALKING. SSS: SELF SELECTED SPEED; L: STEP LENGTH; D: STEP DURATION; θ: HIP ANGLE RANGE.

	SSS (m/s)	L (m)	D (s)	Hip (θ°)
Normal	1.191	1.703	1.43	(-25.4,41.5)
Flexion	1.391	1.684	1.21	(-20.5,52.2)
Extension	1.316	1.408	1.07	(-20.1,42.9)
Both	1.389	1.598	1.15	(-23.4,53.8)

during mid-swing and reduced the max pre-swing extension angle by 4.9°. This agrees with the observations in [47] from experimental tests of bidirectional hip assistance, where hip flexion increased with level of assistance provided. The extension assistance also increased the hip flexion angle slightly (by 1.4°) and decreased the pre-swing extension angle by 5.3°. This decrease in hip extension angle was likely caused by faster walking with a short stride and the absence of extension assistance during the late stance or pre-swing phase. The bidirectional case resulted in a small decrease in extension (2°) while the peak flexion was increased substantially by 12.3°. The effects of hip assistance on the kinematics of the knee joint can be seen in Fig. 4b. The knee angle during normal SSS walking is close to experimentally observed angles [46], except for the delay in flexion at terminal swing. On the other hand, the assistance cases all resulted in straight knee during the majority of the stance phase. In Fig. 5, snapshots of the simulated walking without assistance and with the bidirectional assistance are shown, from which we can clearly see the straight knee phenomenon.

Considering the pattern of biological hip muscle torque [48], we chose the start of offset for extension assistance at the start of LP phase and the start of offset for flexion at the start of the LS. We performed optimizations with the offset time as both an optimization variable and a fixed zero value. At the end, the zero-value offset time gave the better solutions for both unidirectional flexion and extension cases. For both unidirectional cases, the predicted peak torque is very close to 50 Nm. Considering this, we chose to use a fixed peak value (50 Nm) for the bidirectional assistance. Finally, the predicted optimal torque profiles for all three cases were obtained and shown in Fig. 6.

The power generated by the assistive torques for all three cases are presented in Fig.7. As it can be seen, the unidirectional flexion assistance produced large positive hip power around the

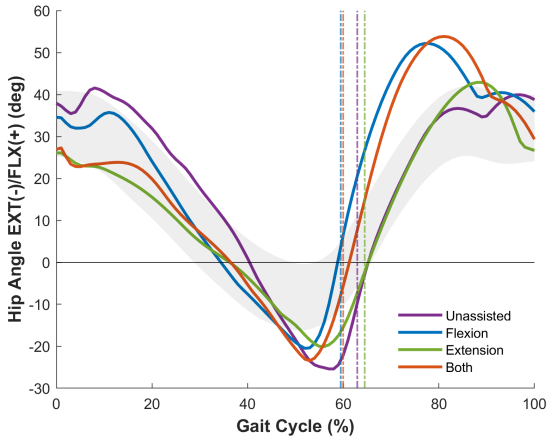

(a)

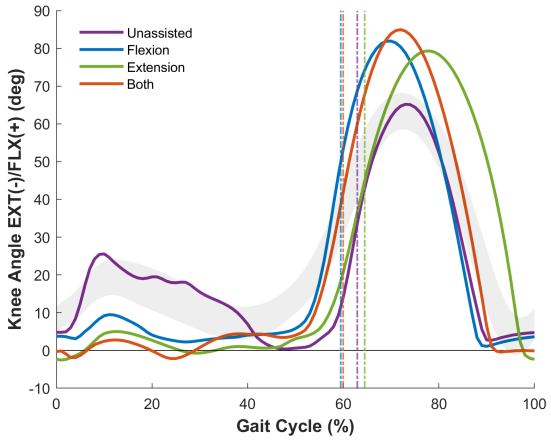

(b)

FIGURE 4: (A) HIP AND (B) KNEE KINEMATICS FOR UNASSISTED AND ASSISTED CASES.VERTICAL LINES INDICATE TOE-OFF (TRANSITION FROM STANCE TO SWING PHASE).

time of toe-off but also produced a smaller amount of negative power before that. The unidirectional extension assistance produced almost only positive power. For the bidirectional assistance, it produced similar large positive work around the time of toe-off to assist flexion and smaller positive power during other periods similar to the extension assistance. Some negative power was also generated by the bidirectional assistance but to a smaller extent in comparison to the flexion assistance. By integrating the power, we were able to obtain the positive, negative, and normalized net work done by the assistances and the results are listed in Table 2. Clearly, flexion assistance generated the largest negative work at 21.01 J whereas the extension assistance generated the least at 0.04 J. The unidirectional flexion and extension as-

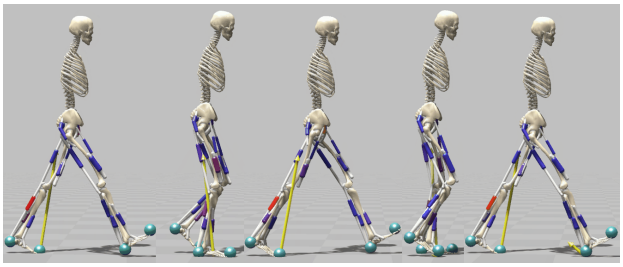

(a)

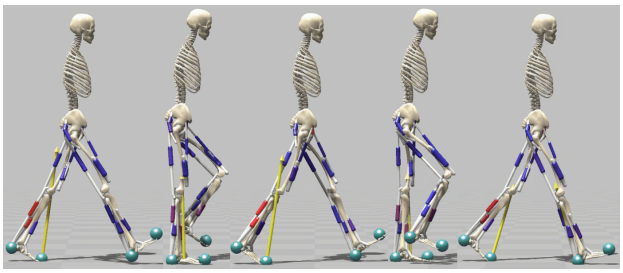

(b)

FIGURE 5: SNAPSHOTS OF WALKING (A) WITHOUT EXOSKELETON ASSISTANCE AND (B) WITH BIDIRECTIONAL HIP ASSISTANCE.

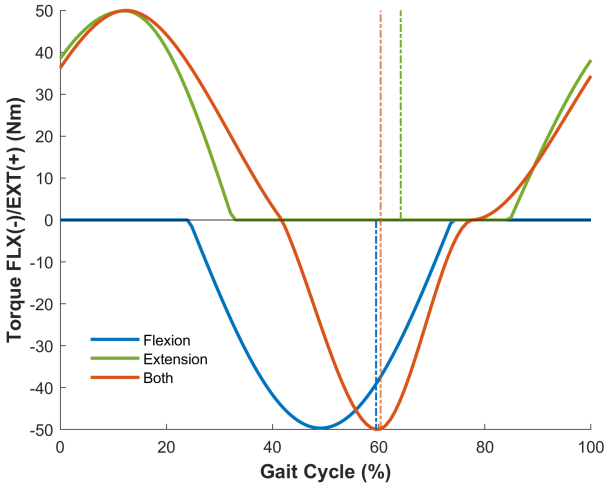

FIGURE 6: THE EXOSKELETON ASSISTANT TORQUE PROFILES FOR FLEXION, EXTENSION, AND BOTH. EACH VERTICAL LINE INDICATES SWING TAKE OFF TIME FOR THE ASSISTANCE OF CORRESPONDING COLOR.

TABLE 2: SUMMARY OF ASSISTIVE POWER AND WORK DELIVERED TO THE HIP JOINT OVER A GAIT CYCLE AND COT SAVINGS. P.W.: POSITIVE WORK; N.W: NEGATIVE WORK.

Case	P.W. (J)	N.W. (J)	Net Work (J/kg/m)	COT (J/kg/m)	Saved (J/kg/m)
NoExo	0	0	0	3.263	-
Flex.	49.82	21.01	0.46	2.638	0.625
Ext.	21.54	0.04	0.41	2.881	0.382
Both	74.79	12.59	1.04	2.523	0.74

sistances generated comparable (normalized) net work (0.46 vs 0.41 $J/kg/m$) while the bidirectional assistance generated more than double of that from either of the unidirectional cases (1.04 $J/kg/m$). The ratios between the negative and positive works are 42.2%, 0.2%, and 16.8%, respectively. Comparing the net work done by the assistances and the COT savings, we found that the flexion assistance produced more COT saving (0.625 $J/kg/m$) than the output of its net work (0.46 $J/kg/m$) by 35.9% while for the other two case the COT savings were lower than the net works. This indicates that the negative work done by the flexion assistance also plays an important role in reducing the COT. Further study of the mechanics and energetics of individual muscles during the negative power period is required to fully understand this behavior.

In Table 2, the COTs for normal walking and assisted walking are listed. The unidirectional assistance reduced the COT by 19.2% for flexion and 11.7% for extension. The bidirectional assistance case reduced the COT by 22.7%, the highest among the three cases. In the work by Kim et al. [49], it was shown that a portable exosuit that assists in extension can reduce the metabolic rate of treadmill walking at 1.5 m/s by 9.3% compared with locomotion without the exosuit. The extension actuation profile applied in this study is similar to ours in trend but with a lower peak torque of 0.5 Nm/kg. In another study by Ding et al. [27], a tethered cable-driven exosuit that provided unidirectional hip extension assistance was able to achieve a metabolic cost reduction of 17.4% at 1.25 m/s by using a human-in-the-loop bayesian optimization protocol, which is higher than our predicted COT saving. The average max force supplied by them is 2.84 N/kg but no moment arm was reported. One noticeable difference of these two studies from ours is that they used the time of maximum hip flexion as the fixed onset timing, which is later than the start of the LP phase we used. The SSS speeds we predicted are closer to the treadmill walking speed in the first study [49] and so is the metabolic cost saving. In another study by Lee et al. [50], a powered bidirectional hip exoskeleton was shown to be able to reduce the COT of walking by 21.1% at a fixed speed

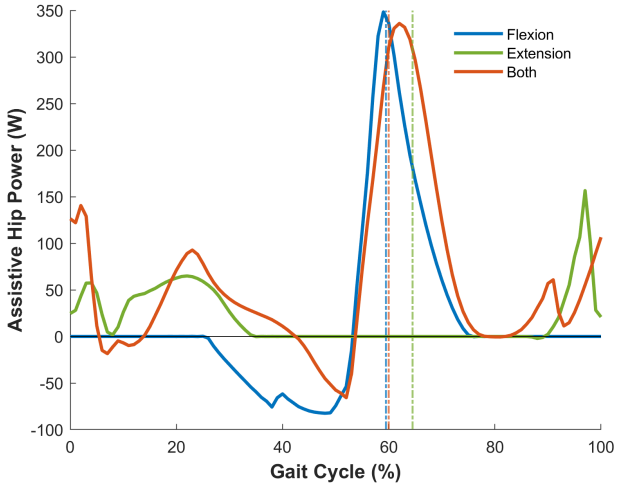

FIGURE 7: THE POWER PRODUCED BY EXOSKELETON ASSISTANCE TORQUES FOR FLEXION, EXTENSION, AND BOTH. EACH VERTICAL LINE INDICATES TOE-OFF FOR THE ASSISTANCE OF CORRESPONDING COLOR.

of 1.16 m/s. With a later version of the same exoskeleton [3], it was shown that a delayed output feedback hip assistance can reduce the COT of walking by 19.8% at a fixed speed of 1.11 m/s. Our modeling results show that it might be possible to achieve even higher COT reduction with optimized assistance.

Predicted muscle activation patterns for the muscles crossing the hip joint are presented in Fig.8 and are compared with EMG on-off timings estimated from [10, 51]. The GMAX was compared to gluteus maximus upper muscle, and the HAMS was compared to a combination of biceps femoris long head, semimembranosus and semitendinosus muscles, while the ILPSO was compared to the intramuscular EMG recordings from the psoas and iliacus [51]. The biarticular RF exhibited very low activation for all simulations and thus is omitted in the figure. The hip flexor ILPSO in our model exhibited moderate activation after ground contact and during LS into early swing in normal SSS walking, which is consistent with the experimental data. Also, activation of ILPSO after ground contact is similar to what was predicted in the simulation studies by Ong et.al [44] and [52]. Flexion assistance decreases the activation of ILPSO while extension assistance increased its activation. The predicted activation timing for the hip extensor groups (GMAX and HAMS) during unassisted SSS walking agree with the simulation results by [53] and [44]. The predicted HAMS muscle activation has a much higher amplitude at the ES phase than that at the LP phase, which differs from experimental EMG measurements that often show comparable amplitudes during these two phases [54]. Similar trend is also observed for the GMAX muscle. One possible

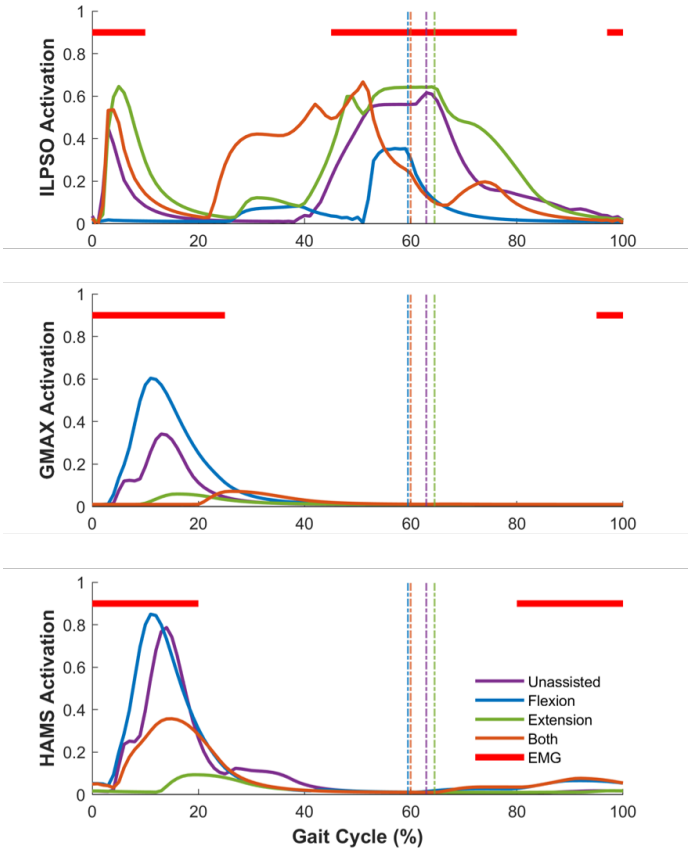

FIGURE 8: PREDICTED MUSCLE ACTIVATION FOR ILPSO, GMAX AND HAMS FOR UNASSISTED AND ASSISTED SCENARIOS. ACTIVATION IS COMPARED TO EXPERIMENTAL MUSCLE EMG ON-OFF TIMING (IN RED) DURING NORMAL WALKING.

reason for this could be the PD control based on the pelvis tilt angle for both muscles. Since the model lacks lumbar joints and back muscles, the regulation of upper body posture falls on the hip muscles. During the ES phase, the hip extensors were likely activated to prevent the torso falling forward. As a result, the predicted muscle hip extension torques during the ES phase were also higher than those computed from experimental motion data. Providing flexion assistance resulted in increased activations in these extensors whereas the extension assistance reduced their activations to a very low level. The bidirectional case reduced the activation levels in the hip extensors to a less degree than the unidirectional extension assistance but interestingly only shifted the activation timing of the ilipsoas without changing the amplitude much.

There are several limitations with the current study. The musculoskeletal model used in our predictive simulations is confined to the sagittal plane like in previous studies [40, 44], has a

rigid foot with locked toes, and lacks upper body degrees of freedom. The use of idealized, massless assistance to the hip is similar to other simulation studies [32, 33] but likely underestimated the burden of wearing a real exoskeleton. Assumptions have also been made regarding the torque profile parameterization, onset timing, and maximum torques of the bidirectional assistance, which may not fully explore the plausible assistance space and result in local optimums. In terms of optimization, the objective function we used may not cover some important aspects of human motion such as reducing fatigue [55]. These limitations may all affect the accuracy of the predicted gait, muscle activation and energetics, and consequently the assistance profiles. Some of these limitations can be addressed straightforwardly and we plan to continue improving the models in future studies.

4. CONCLUSION

Designing wearable exoskeletons is often a trade-off process considering various factors such as power, actuation, cost, weight, and wearability. Knowing how and when to apply assistance to a joint is a critical piece of information for the design. In this study, we demonstrated a predictive modeling and optimization approach to evaluate the effectiveness of hip assistance in human walking and predicted gait adaptation and reduction of COT due to the assistances. We found optimized hip assistance profiles for both unidirectional assistances and bidirectional assistance. The unidirectional hip flexion assistance performed much better than hip extension assistance in terms of COT reduction and caused less changes in gait characteristics (stride length and duration). And the bidirectional hip assistance achieved the greatest reduction in COT (22.7%) and reduced the activations of the hip extensors to a great extent. Our results can provide valuable information for optimal hip actuation (timing and profiles) and help exoskeleton designers make informed decisions. In the future, we would also like to extend the current optimization framework to other joints such as knee, ankle, and the back, also, multi-joint assistance for broader applications.

REFERENCES

[1] Sawicki, G. S., Beck, O. N., Kang, I., and Young, A. J., 2020. "The exoskeleton expansion: improving walking and running economy". *Journal of neuroengineering and rehabilitation,* ***17***(1), pp. 1–9.

[2] Sawicki, G. S., Lewis, C. L., and Ferris, D. P., 2009. "It pays to have a spring in your step". *Exercise and sport sciences reviews,* ***37***(3), p. 130.

[3] Lim, B., Lee, J., Jang, J., Kim, K., Park, Y. J., Seo, K., and Shim, Y., 2019. "Delayed output feedback control for gait assistance with a robotic hip exoskeleton". *IEEE Transactions on Robotics,* ***35***(4), pp. 1055–1062.

[4] Galle, S., Malcolm, P., Collins, S. H., and De Clercq, D., 2017. "Reducing the metabolic cost of walking with an ankle exoskeleton: interaction between actuation timing and power". *Journal of neuroengineering and rehabilitation,* ***14***(1), pp. 1–16.

[5] MacLean, M. K., and Ferris, D. P., 2019. "Energetics of walking with a robotic knee exoskeleton". *Journal of applied biomechanics,* ***35***(5), pp. 320–326.

[6] Umberger, B. R., and Rubenson, J., 2011. "Understanding muscle energetics in locomotion: new modeling and experimental approaches". *Exercise and sport sciences reviews,* ***39***(2), pp. 59–67.

[7] Lenzi, T., Carrozza, M. C., and Agrawal, S. K., 2013. "Powered hip exoskeletons can reduce the user's hip and ankle muscle activations during walking". *IEEE Transactions on Neural Systems and Rehabilitation Engineering,* ***21***(6), pp. 938–948.

[8] McGibbon, C. A., 2003. "Toward a better understanding of gait changes with age and disablement: neuromuscular adaptation". *Exercise and sport sciences reviews,* ***31***(2), pp. 102–108.

[9] Lewis, C. L., and Ferris, D. P., 2008. "Walking with increased ankle pushoff decreases hip muscle moments". *Journal of biomechanics,* ***41***(10), pp. 2082–2089.

[10] Perry, J., and Burnfield, J. M., 2010. "Gait analysis. normal and pathological function 2nd ed". *California: Slack*.

[11] Seo, K., Lee, J., Lee, Y., Ha, T., and Shim, Y., 2016. "Fully autonomous hip exoskeleton saves metabolic cost of walking". In 2016 IEEE International Conference on Robotics and Automation (ICRA), pp. 4628–4635.

[12] Kitatani, R., Ohata, K., Takahashi, H., Shibuta, S., Hashiguchi, Y., and Yamakami, N., 2014. "Reduction in energy expenditure during walking using an automated stride assistance device in healthy young adults". *Archives of physical medicine and rehabilitation,* ***95***(11), pp. 2128–2133.

[13] Sugar, T. G., Fernandez, E., Kinney, D., Hollander, K. W., and Redkar, S., 2017. "Hesa, hip exoskeleton for superior assistance". In *Wearable Robotics: Challenges and Trends*. Springer, pp. 319–323.

[14] Giovacchini, F., Vannetti, F., Fantozzi, M., Cempini, M., Cortese, M., Parri, A., Yan, T., Lefeber, D., and Vitiello, N., 2015. "A light-weight active orthosis for hip movement assistance". *Robotics and Autonomous Systems,* ***73***, pp. 123–134.

[15] Wu, Q., Wang, X., Du, F., and Zhang, X., 2015. "Design and control of a powered hip exoskeleton for walking assistance". *International Journal of Advanced Robotic Systems,* ***12***(3), p. 18.

[16] Yu, S., Huang, T. H., Yang, X., Jiao, C., Yang, J., Chen, Y., Yi, J., and Su, H., 2020. "Quasi-direct drive actuation for a lightweight hip exoskeleton with high backdrivability and high bandwidth". *IEEE/ASME Transactions on Mechatron-*

ics, ***25***(4), pp. 1794–1802.

[17] Lee, Y., Roh, S., Lee, M., Choi, B., Lee, J., Kim, J., Choi, H., Shim, Y., and Kim, Y., 2017. "A flexible exoskeleton for hip assistance". In 2017 IEEE/RSJ International Conference on Intelligent Robots and Systems (IROS), pp. 1058–1063.

[18] Seo, K., Lee, J., and Park, Y. J., 2017. "Autonomous hip exoskeleton saves metabolic cost of walking uphill". In 2017 International Conference on Rehabilitation Robotics (ICORR), pp. 246–251.

[19] Perera, U., Dasanayake, N., Hettiarachchi, H., Mannapperuma, M., Ranaweera, R., and Gopura, R., 2020. "Hipexo: A hip exoskeleton robot for load lifting with flexible trunk linkage mechanism". In 2020 Moratuwa Engineering Research Conference (MERCon), IEEE, pp. 614–619.

[20] Lewis, C. L., and Ferris, D. P., 2011. "Invariant hip moment pattern while walking with a robotic hip exoskeleton". *Journal of biomechanics,* ***44***(5), pp. 789–793.

[21] Quinlivan, B. T., Lee, S., Malcolm, P., Rossi, D. M., Grimmer, M., Siviy, C., Karavas, N., Wagner, D., Asbeck, A., Galiana, I., and Walsh, C. J., 2017. "Assistance magnitude versus metabolic cost reductions for a tethered multiarticular soft exosuit". *Science Robotics,* ***2***(2), p. eaah4416.

[22] Do Nascimento, B. G., Vimieiro, C. B. S., Nagem, D. A. P., and Pinotti, M., 2008. "Hip orthosis powered by pneumatic artificial muscle: voluntary activation in absence of myoelectrical signal". *Artificial organs,* ***32***(4), pp. 317–322.

[23] Kawamura, T., Takanaka, K., Nakamura, T., and Osumi, H., 2013. "Development of an orthosis for walking assistance using pneumatic artificial muscle: A quantitative assessment of the effect of assistance". In 2013 IEEE 13th International Conference on Rehabilitation Robotics (ICORR), IEEE, pp. 1–6.

[24] Jin, S., Iwamoto, N., Hashimoto, K., and Yamamoto, M., 2017. "Experimental evaluation of energy efficiency for a soft wearable robotic suit". *IEEE Transactions on Neural Systems and Rehabilitation Engineering,* ***25***(8), pp. 1192–1201.

[25] Choe, D., Kim, J., Lee, G., Karavas, N., Menard, N., and Walsh, C., 2017. "Autonomous soft exosuit with hip extension assistance for overground walking and jogging". In 2017 International Symposium on Wearable Robotics and Rehabilitation (WeRob), pp. 1–1.

[26] Ding, Y., Panizzolo, F. A., Siviy, C., Malcolm, P., Galiana, I., Holt, K. G., and Walsh, C. J., 2016. "Effect of timing of hip extension assistance during loaded walking with a soft exosuit". *Journal of neuroengineering and rehabilitation,* ***13***(1), pp. 1–10.

[27] Ding, Y., Kim, M., Kuindersma, S., and Walsh, C. J., 2018. "Human-in-the-loop optimization of hip assistance with a soft exosuit during walking". *Science Robotics,* ***3***(15), p. eaar5438.

[28] Asbeck, A. T., Schmidt, K., and Walsh, C. J., 2015. "Soft exosuit for hip assistance". *Robotics and Autonomous Systems,* ***73***, pp. 102 – 110. Wearable Robotics.

[29] Zhang, J., Fiers, P., Witte, K. A., Jackson, R. W., Poggensee, K. L., Atkeson, C. G., and Collins, S. H., 2017. "Human-in-the-loop optimization of exoskeleton assistance during walking". *Science,* ***356***(6344), pp. 1280–1284.

[30] Jackson, R. W., Dembia, C. L., Delp, S. L., and Collins, S. H., 2017. "Muscle–tendon mechanics explain unexpected effects of exoskeleton assistance on metabolic rate during walking". *Journal of Experimental Biology,* ***220***(11), pp. 2082–2095.

[31] Grabke, E. P., Masani, K., and Andrysek, J., 2019. "Lower limb assistive device design optimization using musculoskeletal modeling: A review". *Journal of Medical Devices,* ***13***(4).

[32] Dembia, C. L., Silder, A., Uchida, T. K., Hicks, J. L., and Delp, S. L., 2017. "Simulating ideal assistive devices to reduce the metabolic cost of walking with heavy loads". *PloS one,* ***12***(7), p. e0180320.

[33] Uchida, T. K., Seth, A., Pouya, S., Dembia, C. L., Hicks, J. L., and Delp, S. L., 2016. "Simulating ideal assistive devices to reduce the metabolic cost of running". *PloS one,* ***11***(9), p. e0163417.

[34] Zhou, X., 2020. "Predictive human-in-the-loop simulations for assistive exoskeletons". In ASME 2020 International Design Engineering Technical Conferences and Computers and Information in Engineering Conference, American Society of Mechanical Engineers Digital Collection.

[35] Zhou, X., and Chen, X., 2020. "Design and evaluation of torque compensation controllers for a lower extremity exoskeleton". *Journal of Biomechanical Engineering,* ***143***(1).

[36] Geijtenbeek, T., 2019. "Scone: Open source software for predictive simulation of biological motion". *Journal of Open Source Software,* ***4***(38), p. 1421.

[37] Dembia, C. L., Bianco, N. A., Falisse, A., Hicks, J. L., and Delp, S. L., 2020. "Opensim moco: musculoskeletal optimal control". *PLOS Computational Biology,* ***16***(12), p. e1008493.

[38] Seth, A., Hicks, J. L., Uchida, T. K., Habib, A., Dembia, C. L., Dunne, J. J., Ong, C. F., DeMers, M. S., Rajagopal, A., Millard, M., et al., 2018. "Opensim: Simulating musculoskeletal dynamics and neuromuscular control to study human and animal movement". *PLoS computational biology,* ***14***(7), p. e1006223.

[39] Millard, M., Uchida, T., Seth, A., and Delp, S. L., 2013. "Flexing computational muscle: modeling and simulation of musculotendon dynamics". *Journal of biomechanical engineering,* ***135***(2).

[40] Geyer, H., and Herr, H., 2010. "A muscle-reflex model that encodes principles of legged mechanics produces hu-

man walking dynamics and muscle activities". *IEEE Transactions on neural systems and rehabilitation engineering,* ***18***(3), pp. 263–273.

[41] Sherman, M. A., Seth, A., and Delp, S. L., 2011. "Simbody: multibody dynamics for biomedical research". *Procedia Iutam,* ***2***, pp. 241–261.

[42] Hansen, N., Müller, S. D., and Koumoutsakos, P., 2003. "Reducing the time complexity of the derandomized evolution strategy with covariance matrix adaptation (cma-es)". *Evolutionary computation,* ***11***(1), pp. 1–18.

[43] Wang, J. M., Hamner, S. R., Delp, S. L., and Koltun, V., 2012. "Optimizing locomotion controllers using biologically-based actuators and objectives". *ACM Transactions on Graphics (TOG),* ***31***(4), pp. 1–11.

[44] Ong, C. F., Geijtenbeek, T., Hicks, J. L., and Delp, S. L., 2019. "Predicting gait adaptations due to ankle plantarflexor muscle weakness and contracture using physics-based musculoskeletal simulations". *PLoS computational biology,* ***15***(10), p. e1006993.

[45] Uchida, T. K., Hicks, J. L., Dembia, C. L., and Delp, S. L., 2016. "Stretching your energetic budget: how tendon compliance affects the metabolic cost of running". *PloS one,* ***11***(3), p. e0150378.

[46] Bovi, G., Rabuffetti, M., Mazzoleni, P., and Ferrarin, M., 2011. "A multiple-task gait analysis approach: kinematic, kinetic and emg reference data for healthy young and adult subjects". *Gait & posture,* ***33***(1), pp. 6–13.

[47] Kang, I., Hsu, H., and Young, A., 2019. "The effect of hip assistance levels on human energetic cost using robotic hip exoskeletons". *IEEE Robotics and Automation Letters,* ***4***(2), pp. 430–437.

[48] Grimmer, M., Eslamy, M., and Seyfarth, A., 2014. "Energetic and peak power advantages of series elastic actuators in an actuated prosthetic leg for walking and running". In Actuators, Vol. 3, Multidisciplinary Digital Publishing Institute, pp. 1–19.

[49] Kim, J., Lee, G., Heimgartner, R., Revi, D. A., Karavas, N., Nathanson, D., Galiana, I., Eckert-Erdheim, A., Murphy, P., Perry, D., et al., 2019. "Reducing the metabolic rate of walking and running with a versatile, portable exosuit". *Science,* ***365***(6454), pp. 668–672.

[50] Lee, J., Seo, K., Lim, B., Jang, J., Kim, K., and Choi, H., 2017. "Effects of assistance timing on metabolic cost, assistance power, and gait parameters for a hip-type exoskeleton". In 2017 International Conference on Rehabilitation Robotics (ICORR), IEEE, pp. 498–504.

[51] Andersson, E. A., Nilsson, J., and Thorstensson, A., 1997. "Intramuscular emg from the hip flexor muscles during human locomotion". *Acta Physiologica Scandinavica,* ***161***(3), pp. 361–370.

[52] John, C. T., Anderson, F. C., Higginson, J. S., and Delp, S. L., 2013. "Stabilisation of walking by intrinsic muscle properties revealed in a three-dimensional muscle-driven simulation". *Computer methods in biomechanics and biomedical engineering,* ***16***(4), pp. 451–462.

[53] Dorn, T. W., Wang, J. M., Hicks, J. L., and Delp, S. L., 2015. "Predictive simulation generates human adaptations during loaded and inclined walking". *PloS one,* ***10***(4), p. e0121407.

[54] Arnold, E. M., Hamner, S. R., Seth, A., Millard, M., and Delp, S. L., 2013. "How muscle fiber lengths and velocities affect muscle force generation as humans walk and run at different speeds". *Journal of Experimental Biology,* ***216***(11), pp. 2150–2160.

[55] Falisse, A., Serrancolí, G., Dembia, C. L., Gillis, J., Jonkers, I., and De Groote, F., 2019. "Rapid predictive simulations with complex musculoskeletal models suggest that diverse healthy and pathological human gaits can emerge from similar control strategies". *Journal of The Royal Society Interface,* ***16***(157), p. 20190402.